Refractive Plasmonic Sensor Based on Fano Resonances in an Optical System *

Wei-Jie Mai(买威洁)[1,2], Yi-Lin Wang(王艺霖)[1,2], Yun-Yun Zhang(张云云)[1,2], Lu-Na Cui(崔鲁娜)[1,2], Li Yu(于丽)[1,2]**

[1]State Key Laboratory of Information Photonics and Optical Communications, Beijing University of Posts and Telecommunications, Beijing 100876

[2]School of Science, Beijing University of Posts and Telecommunications, Beijing 100876

(Received 23 September 2016)

A symmetric plasmonic structure consisting of metal–insulator–metal waveguide, groove and slot cavities is studied, which supports double Fano resonances deriving from two different mechanisms. One of the Fano resonances originates from the interference between the resonances of groove and slot cavities, and the other comes from the interference between slot cavities. The spectral line shapes and the peaks of the double Fano resonances can be modulated by changing the length of the slot cavities and the height of the groove. Furthermore, the wavelength of the resonance peak has a linear relationship with the length of the slot cavities. The proposed plasmonic nanosensor possesses a sensitivity of 800 nm/RIU and a figure of merit of 3150, which may have important applications in switches, sensors, and nonlinear devices.

PACS: 42.82.Et, 52.25.Fi, 42.82.Gw DOI: 10.1088/0256-307X/34/2/024204

Fano resonance arises from the coherent coupling and interference between a discrete state and a continuous state, which possesses a distinctly asymmetric line shape. Recently, the Fano resonance in plasmonic structure has aroused much attention since surface plasmon polaritons (SPPs) can overcome the diffraction limit and confine the light in sub-wavelength dimensions.[1] Various plasmonic structures have been designed to achieve the Fano resonance.[2–4] A common way to obtain the Fano resonance is using the asymmetric plasmonic structure, such as the symmetry-breaking T-shape double slit,[5] the broken symmetry in disk cavities or the ring,[6,7] asymmetric stub pair in metal–insulator–metal (MIM) waveguide and asymmetric plasmonic nano-particle clusters.[8–10] Moreover, the Fano resonance can also be realized through symmetric plasmonic structures, including cavity–cavity interference,[11–13] nanoslits in a metallic membrane,[14] waveguide-coupled resonators and the coupling of plasmonic nanoclusters.[15–17] Due to the great sensitivity and large figure of merit (FOM) of the device based on the unique line shape, the Fano resonance can be easily achieved, which has shown great potential in sensors, switches, nonlinear and slow light areas.[18–20] Moreover, multiple Fano resonances have received much attention for the potential application in the enhanced biochemical sensing, spectroscopy, and multicolor nonlinear processes.[21–24]

In this Letter, a metal–insulator–metal (MIM) waveguide structure is proposed to realize the double Fano resonances in a symmetric plasmonic structure. In the symmetric plasmonic structure, a couple of slot-cavity resonators are placed close to the ends of the groove. Two identical barriers are distributed adjacent to the edges of the groove, which symmetrically locate at both sides of an MIM bus waveguide. When the propagating SPPs transmit in the groove, partial energy of SPPs couples into the groove and the slot cavities. The interference between groove and slot cavities results in the double Fano resonances. It is also found that the Fano resonance line shape and the peak wavelength strongly depend on the refractive index in the groove and the lengths of the slot cavities. The proposed plasmonic structure has an excellent sensitivity with 800 nm/RIU and FOM 3150. Our proposed structure can give some reference for designs of plasmonic switches, filters and enhanced bio-chemical sensors.

The proposed MIM waveguide structure is shown in Fig. 1. The groove locates in the center of the structure, and the left and right sides are the input and the output bus waveguides, respectively. The two slot cavities locate on the upper and the lower sides of the groove, which act as the Fabry–Perot (FP) resonators.

The length and the height of the groove are denoted as W and H, respectively. The coupling distances from the groove to the input/output buses and from the groove to the slot cavities are d and g, respectively, and W_1 and L are the width and length of the slot cavities, respectively, and W_2 represents the widths of the buses. Here the insulators are chosen to be air ($n = 1.0$) in the waveguide and cavity. The metal is assumed as silver, whose frequency-dependent complex relative permittivity is characterized by the Drude model,

$$\varepsilon_{\mathrm{m}}(\omega) = \varepsilon_{\infty} - \omega_{\mathrm{p}}/[\omega(\omega + i\gamma)], \quad (1)$$

where ε_{∞} is the dielectric constant at the infinite frequency, ω_{p} and γ represent the bulk plasma frequencies and the electron collision, respectively, and ω is

*Supported by the Ministry of Science and Technology of China under Grant No 2016YFA0301300, the National Natural Science Foundation of China under Grant Nos 11374041 and 11574035, and the State Key Laboratory of Information Photonics and Optical Communications.

**Corresponding author. Email: yuliyuli@bupt.edu.cn

© 2017 Chinese Physical Society and IOP Publishing Ltd

the angular frequency of incident light. The parameters for silver can be set as $\varepsilon_\infty = 3.7$, $\omega_p = 9.1\,\text{eV}$ and $\gamma = 0.018\,\text{eV}$.[25] To excite the SPPs, the transverse magnetic (TM) plane wave was set as the input source.

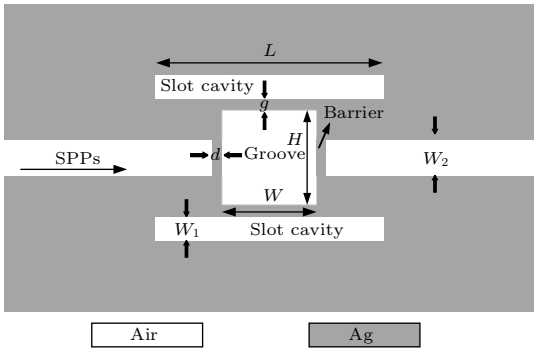

Fig. 1. Sketch of the symmetric plasmonic structure based on the MIM waveguide.

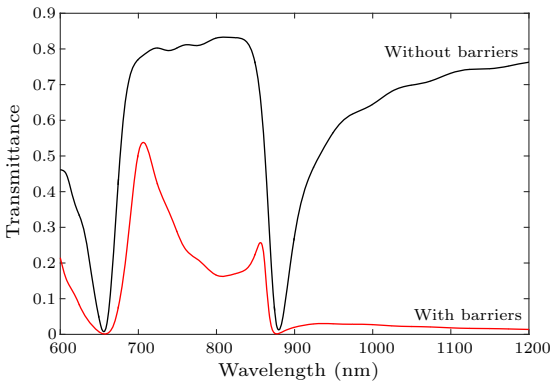

Fig. 2. The transmittance of the plasmonic structure with parameters $L = 550\,\text{nm}$, $W_1 = 50\,\text{nm}$, $W_2 = 50\,\text{nm}$, $d = 10\,\text{nm}$, $H = 200\,\text{nm}$, $W = 200\,\text{nm}$, and $g = 10\,\text{nm}$.

The transmittance of the proposed plasmonic structure is simulated and researched by using commercial software (COMSOL Multiphysics). The transmittance is defined to be $T = p_{\text{out}}/p_{\text{in}}$, where p_{out} and p_{in} represent the power flow of the out field and incident field, respectively.

Figure 2 shows the transmittance of the plasmonic structure with and without barriers. The parameters of the structure are $L = 550\,\text{nm}$, $W_1 = 50\,\text{nm}$, $W_2 = 50\,\text{nm}$, $d = 10\,\text{nm}$, $H = 200\,\text{nm}$, $W = 200\,\text{nm}$, and $g = 10\,\text{nm}$. The figure shows the distinct asymmetrical double Fano resonances profile, which differs from the Lorentzian resonance. We call the left Fano resonance FR_1, and the right Fano resonance is FR_2. It is worth noting that the Fano line shapes of FR_1 and FR_2 possess opposite directions, which results from different phase shifts of the resonance mode. When the barriers exist, only partial energy of SPPs can couple into the groove and the transmittance will decrease. Interestingly, the positions of the dips have almost no change with or without barriers. We attribute the phenomenon to the destructive interference.

Figure 3 depicts the distribution of the normalized z-direction magnetic field $|H_z|^2$ at the wavelengths 705 nm and 858 nm, corresponding to the resonance wavelengths of FR_1 and FR_2, respectively. The distribution $|H_z|^2$ at the wavelength 705 nm shows the interference between the groove resonance and the fourth-order resonance of the two identical slot cavities, which is the origin of FR_1. The distribution $|H_z|^2$ at the wavelength 858 nm shows the interference of three-order resonance in the two slot cavities, which is the source of FR_2. The distributions of the normalized z-direction magnetic field $|H_z|^2$ at the wavelengths 656 nm and 876 nm at the dip are also shown in Fig. 3.

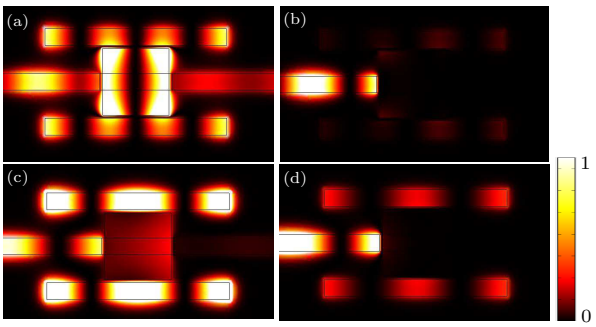

Fig. 3. The distribution of the normalized z-direction magnetic field $|H_z|^2$ at the wavelengths: (a) 705 nm, (b) 656 nm, (c) 858 nm and (d) 876 nm.

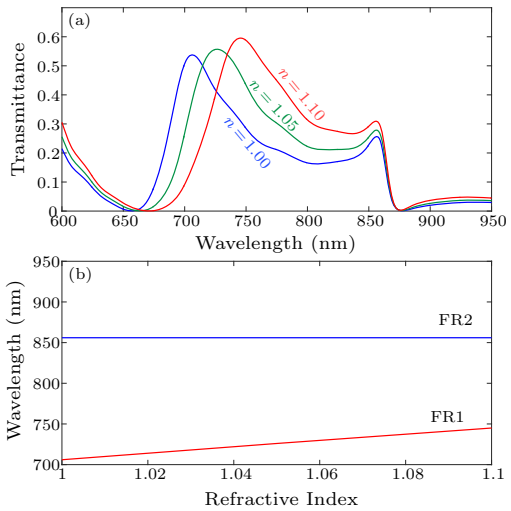

Fig. 4. (a) The transmission spectra of the plasmonic structure with different refractive indexes of the insulators in the groove. (b) With the increasing refractive index from 1.0 to 1.1, both peak positions of FR_1 and FR_2 shift to red and show the linear relationship.

We adjust the refractive index of groove from 1.0 to 1.1, the peak position of FR_1 is red shifted and displays the nearly linear relationships, as shown in Fig. 4. However, the peak position of the FR_2 is almost unchanged, which derives from interference between slot cavities.

Sensing is an important application of the Fano resonance, thus we study the performance of our proposed structure as a plasmonic nanosensor. The FOM as a key parameter is widely used to evaluate the performance of the double Fano resonances. The FOM is

defined as[26]

$$\mathrm{FOM} = \max\left|\frac{dT(\lambda)/dn(\lambda)}{T(\lambda)}\right|, \quad (2)$$

where $T(\lambda)$ is the transmittance at the specific wavelength, $dT(\lambda)/dn(\lambda)$ is the transmittance change at the fixed wavelength induced by a refractive index change, and λ_0 corresponds to the wavelength when FOM reaches the maximum value. Figure 5(a) depicts the transmission spectra for different refractive indexes of the insulator in the waveguide, the groove and the two identical slot cavities. The sensitivity (nm/RIU) is defined as the shift in the resonance wavelength per unit change of the refractive index. Figure 5(b) shows the peak positions of FR_1 and FR_2 changing with the refractive index of the insulator. With increasing the refractive index from 1.0 to 1.1, the peak positions of FR_1 and FR_2 both shift to red and show the linear relationship. The sensitivity has a high value about 800 nm/RIU, which is excellent compared with the existing results.[27] Figure 6 shows the FOM curve and the transmission spectrum with the structure parameters of $L = 550$ nm, $W_1 = 50$ nm, $W_2 = 50$ nm, $d = 10$ nm, $H = 200$ nm, $W = 200$ nm, and $g = 10$ nm. The maximum FOM of our proposed nanosensor is about 3150.

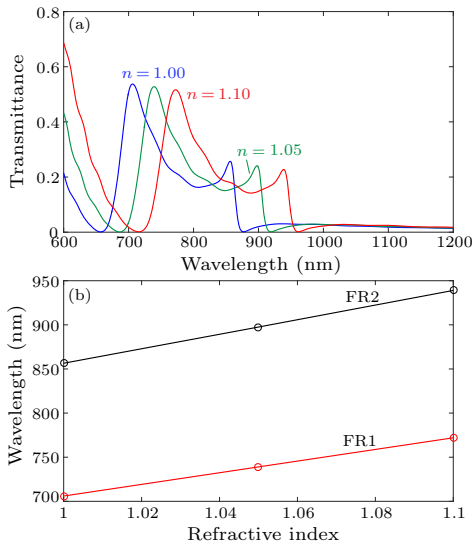

Fig. 5. (a) The transmission spectra for different refractive indexes of the insulator in the waveguide, the groove and the two identical slot cavities. (b) With the increasing refractive index from 1.0 to 1.1, the peak positions of FR_1 and FR_2 shift to red and show the linear relationship.

Also, we investigate the change of transmittance with the growth of L. When L increases from 500 nm to 600 nm, the peak position of FR_1 red shifts from 704 nm to 776 nm and the peak position of FR_2 red shifts from 855 nm to 1060 nm, as shown in Fig. 7.

We fix the length $L = 550$ nm and change the groove height H from 200 nm to 300 nm. The peak position of the FR_1 changes greatly, while the change of the FR_2 position is only about 10 nm, as shown in Fig. 8. This is because the origination of FR_1 is related to the groove, while FR_2 mainly originates from the coupling between the two slot cavities.

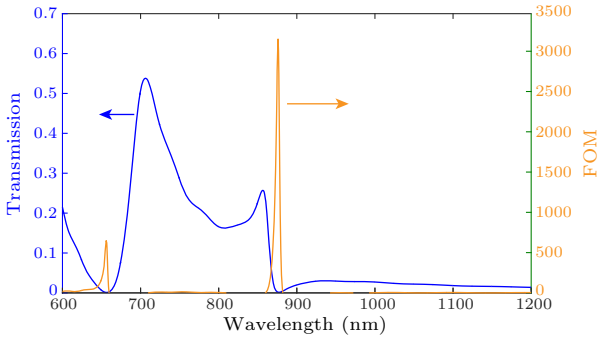

Fig. 6. The FOM curve and the transmission spectrum with the proposed structure parameters of $L = 550$ nm, $W_1 = 50$ nm, $W_2 = 50$ nm, $d = 10$ nm, $H = 200$ nm, $W = 200$ nm, and $g = 10$ nm.

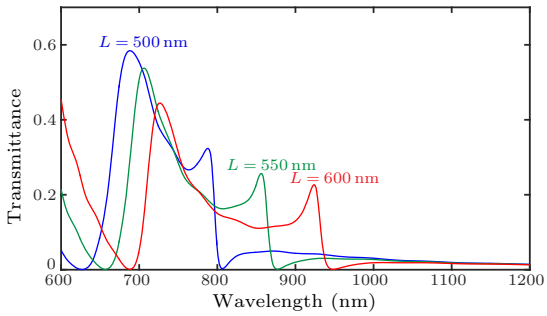

Fig. 7. With L increasing from 500 nm to 650 nm, the peak positions of the FR_1 and FR_2 both change.

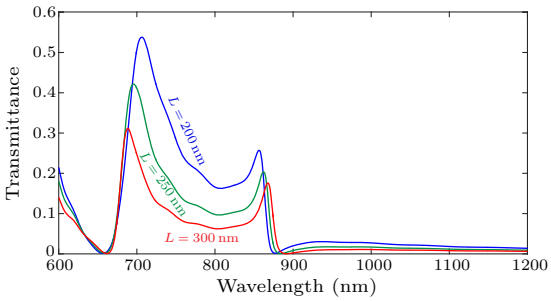

Fig. 8. The changing of the peak positions of the FR_1 and FR_2 with H increasing from 200 nm to 300 nm.

Compared with Ref. [11], this study has more interesting results. By adding the silver barriers, we obtain two asymmetric Fano resonance profiles, which originate from the interference between the groove and the slot cavities and the interference of three-order resonance in the two slot cavities, respectively. However, Wen *et al.*[11] obtained the Fano resonance profile by using the interaction of the broad bright mode and the narrow mode. Furthermore, we analyze the origin of the two peaks of the Fano resonances. Double Fano resonances can provide two transmission windows. We can switch between the two resonances, which can provide flexibility in tuning the resonant wavelengths or sensing and has gained much attention for the advantages in the enhanced bio-chemical sensing, spectroscopy, and multicolor nonlinear processes.[28]

In summary, the double Fano resonances have been demonstrated in our proposed MIM waveguide structure, composed of two identical buses, the groove and the slot cavities. The double Fano resonances originate from two different mechanisms. One of the Fano resonances originates from the interference between groove and the slot cavities. The other results from the interference of the slot cavities. The spectral line shape and the peak of the double Fano resonances can be modulated by changing the length of the slot cavities and the height of the groove. Furthermore, the wavelength of the resonance peak has a linear relationship with the length of the slot cavities. The proposed plasmonic structure possesses a sensitivity of 800 nm/RIU and an FOM of 3150. Due to these excellent performances, the double Fano resonances can be used as switches, filters and enhanced bio-chemical sensors.

References

[1] Barnes W L, Dereux A and Tw E 2003 *Nature* **424** 824
[2] Shang C, Chen Z, Wang L L, Zhao Y F, Duan G Y and Yu L 2014 *Chin. Phys. Lett.* **31** 114202
[3] Zhang X Y, Wang L L, Chen Z, Cui L N, Shang C, Zhao Y F, Duan G Y, Liu J B and Yu L 2015 *Chin. Phys. Lett.* **32** 054209
[4] Yun B, Hu G, Zhang R and Cui Y 2016 *J. Opt.* **18** 055002
[5] Chen J, Li Z, Zou Y, Deng Z, Xiao J and Gong Q 2013 *Plasmonics* **8** 1627
[6] Lassiter J B, Sobhani H, Fan J A, Kundu J, Capasso F, Nordlander P and Halas N J 2010 *Nano Lett.* **10** 3184
[7] Hao F, Sonnefraud Y, Van D P, Maier S A, Halas N J and Nordlander P 2008 *Nano Lett.* **8** 3983
[8] Qi J, Chen Z, Jing C, Li Y, Qiang W, Xu J and Suan Q 2014 *Opt. Express* **22** 14688
[9] Chen Z Q, Qi J W, Chen J, Li Y D, Hao Z Q, Lu W Q, Xu J J and Sun Q 2013 *Chin. Phys. Lett.* **30** 057301
[10] Shegai T, Chen S, Miljkovi V D, Zengin G, Johansson P and Kall M 2011 *Nat. Commun.* **2** 481
[11] Wen K, Hu Y, Chen L, Zhou J, Lei L and Guo Z 2015 *Plasmonics* **10** 27
[12] Lu H, Liu X, Mao D, Gong Y and Wang G 2011 *Opt. Lett.* **36** 3233
[13] Lu H, Liu X, Mao D and Wang G 2012 *Opt. Lett.* **37** 3780
[14] Collin S, Vincent G, Haidar R, Bardou N, Rommeluere S and Pelouard J L 2010 *Phys. Rev. Lett.* **104** 027401
[15] Zhang C X, Nie Y H and Liang J Q 2008 *Chin. Phys.* B **17** 2670
[16] Fan J A, Wu C, Bao K, Bao J, Bardhan R, Halas N J, Manoharan V N, Nordlander P, Shvets G and Capasso F 2010 *Science* **328** 1135
[17] Lassiter J B, Sobhani H, Knight M W, Mielczarek W S, Nordlander P and Halas N J 2012 *Nano Lett.* **12** 1058
[18] Verellen N, Sonnefraud Y, Sobhani H, Hao F Moshchalkov V V, Dorpe P V, Nordlander P and Maier S A 2009 *Nano Lett.* **9** 1663
[19] Miroshnichenko A E, Flach S and Kivshar Y S 2010 *Rev. Mod. Phys.* **82** 2257
[20] Chen J, Li Z, Zhang X, Xiao J and Gong Q 2013 *Sci. Rep.* **3** 1451
[21] Guevara M L L D, Claro F and Orellana P A 2003 *Phys. Rev.* B **67** 195335
[22] Wu C, Khanikaev A B and Shvets G 2011 *Phys. Rev. Lett.* **106** 107403
[23] Eickhoff C, Teichmann M and Weinelt M 2011 *Phys. Rev. Lett.* **107** 176804
[24] Shuai Y, Zhao D, Singh Chadha A, Seo J H, Yang H, Fan S, Ma Z and Zhou W 2013 *Appl. Phys. Lett.* **103** 241106
[25] Han Z and Si B 2011 *Opt. Express* **19** 3251
[26] Becker J, Trügler A, Jakab A, Hohenester U and Sonnnichsen C 2010 *Plasmonics* **5** 161
[27] Liu N, Weiss T and Mesch M 2010 *Nano Lett.* **10** 1103
[28] Li S, Zhang Y, Song X, Wang Y and Yu L 2016 *Opt. Express* **24** 15351